Design considerations for a 50-watt cw, fundamental mode, diode-pumped solid-state laser

R.J. Shine Jr., T.C. Merrill, A.J. Alfrey, E.K. Gustafson, and R.L. Byer

E. L. Ginzton Laboratory
Stanford University
Stanford, California 94305

ABSTRACT

Advances in diode laser arrays have made possible diode-pumped solid-state lasers with output powers approaching those of lamp-pumped lasers. The spectral overlap between the output of diode lasers and the absorption bands of solid-state laser materials leads to significant improvements in pumping efficiency and hence decreases the thermal loading compared to lamp-pumped lasers of equal output power. Nevertheless, for high power cw applications, thermal management is still a significant problem. Thermal lensing and stress induced birefringence can degrade the beam quality of the laser, and in some cases extreme thermal loading can lead to fracture of the laser material. Our research involves designing and building an efficient diode-pumped solid-state laser with 50 watts of cw output power in a single-frequency, diffraction-limited, stable-unstable resonator fundamental mode. Both thermal management issues and careful resonator design are important in achieving this goal.

To achieve the design goal of 50 watts cw in a single-frequency, fundamental mode we have chosen a slab laser design. The slab geometry with a zig-zag optical path eliminates stress birefringence and thermal focusing to first order in a uniformly pumped, ideal slab. However, at the thermal loads we are considering, higher order effects become significant. We have developed a computer program to analyze the full three dimensional behavior of the thermally loaded slab and have used this code in an attempt to minimize the wavefront distortion of a beam as it traverses the slab.

The resonator design is also critical in achieving single-frequency, fundamental mode operation with high extraction efficiency. Because of the rectangular geometry and size of the slab laser, we have chosen to build a stable-unstable resonator. Single frequency operation will be obtained by injection locking a ring cavity. Mode selection is achieved in the wide transverse direction of the slab by using an unstable cavity with a super-Gaussian mirror. An unstable resonator supports large mode volumes and has large discrimination against higher order transverse modes. In addition, a super-Gaussian mirror profile provides efficient extraction in a high quality mode. Our resonator design should lead to efficient operation in a near TEM_{00} mode with a slope efficiency approaching those of slab lasers with multimode output.

Slab laser designs are easily scaled to higher output powers. Using the considerations discussed below, it should be possible to build a few hundred watt cw, diffraction-limited, stable-unstable resonator fundamental mode solid-state laser in the near future. The cost of high-power laser-diode arrays is the major obstacle at the present time.

1. INTRODUCTION

One of the goals of the laser development program at Stanford is to design and build a laser that meets the laser design specifications for the Laser Interferometer Gravity-Wave Observatory (LIGO) program.[1] This application places several requirements on the laser. First, reliable around-the-clock operation is necessary. Second, an efficient system is desired to reduce operating costs. Third, a high power cw source is needed to improve the signal-to-noise ratio for the gravity-wave detector. And fourth, the mode quality is critically important since the laser will be frequency locked to a standing-wave cavity; the laser mode should match the interferometer cavity mode for efficient coupling into the high finesse cavities which act as the arms of the interferometer. A frequency stabilized, 50 watt cw, fundamental mode solid-state laser that can be doubled to the green would be useful for the next stage of development of the LIGO program. In addition to demonstrating a source for the LIGO program, a 50 watt cw, fundamental mode, single-frequency laser has applications in non-linear frequency conversion, space-based

0-8194-1092-6/93/$6.00

coherent communications, and global wind sensing. However, the design of this laser requires some work to minimize thermal effects and to obtain high beam quality.

The laser being built at Stanford will use 250 watts of laser diode pump power, which will be coupled to the gain medium through optical fibers, with each fiber delivering 10 watts of power.[2] We have chosen to fiber couple the diode pump sources to improve reliability and maintainability as well as to simplify the design and thermal control. Since the laser must be able to operate around-the-clock, we need a soft failure mode with easy repair and replacement should a diode laser fail. With fiber coupling, the laser head and the pump sources are isolated from each other, and a pump diode can be easily replaced. When a diode fails, the laser output power should drop by only a few percent due to the decrease in pump power and so the laser will not need to be shut down when a diode is replaced.

We have chosen to use YAG as the laser host due to its high optical quality and excellent thermal characteristics. YAG is isotropic and has one of the higher thermal shock parameters available for materials which can be diode-pumped.[3] This permits a higher thermal loading before stress fracture occurs. In the design of high power solid-state lasers, thermal management is of primary concern.

2. THERMAL AND STRESS CONSIDERATIONS

Most Nd:YAG lasers use rods as the active media. A rod is easy to fabricate and mount, allows efficient end pumping, and produces a spherical output beam. However, in high power applications the rod geometry suffers from thermal lensing and stress-induced birefringence.[4] These problems are overcome to first order by using a zig-zag slab geometry.[5]

Consider a rod with uniform pump distribution and surface cooling. The steady-state solution of the heat equation yields a radial temperature profile which is quadratic. The temperature profile is

$$T(r) = T(r_0) + \left(\frac{Q}{4K}\right)(r_0^2 - r^2),$$

where Q is the heat deposited per unit volume and K is the thermal conductivity of the material. The heat deposited per unit volume is a function of the absorbed pump power. The temperature difference between the rod center and the edge is

$$T(0) - T(r_0) = \frac{P_a}{4\pi KL},$$

where P_a is the absorbed pump power and L is the rod length. This temperature profile leads to both thermal lensing and thermally induced stresses. The thermal lensing arises mostly from the temperature dependence of the refractive index, dn/dt. (This assumes $dn/dt \neq 0$, which is valid for most laser crystals.) A quadratic temperature profile produces a quadratic index variation which acts as a simple spherical lens. This thermal lensing can be compensated for by careful resonator design, adding focusing elements into the cavity, or by grinding correcting surfaces onto the ends of the rod. A more complicated situation is created if the pump power deposition is not uniform in the rod. At high thermal loads aspheric correction is necessary. However, a more severe problem is caused by the thermal stresses.

The thermal stresses arise because the hotter central region of the rod is constrained from expansion by the cooler surface region. This thermally induced stress leads to stress birefringence in the rod through the photoelastic effect, which generates a refractive index variation from the strain in the rod.[4] The cylindrical geometry of the rod results in principal axes of the induced birefringence oriented in the radial and tangential directions. Hence, a linearly polarized beam will suffer a position-dependent depolarization in a rod. On the principal axes the stress birefringence will act as a phase retarder; the linear polarization is oriented along only one of the radial or tangential principal axes. However, at all other positions in the rod, the stress birefringence will cause the incident linearly polarized light to emerge with elliptical polarization. If the beam is passed through a polarizing element, an isogyre pattern will be observed. Since polarized light is necessary for many applications, such as non-linear optics and electro-optic Q-switching, stress birefringence decreases the useful output power of a high power rod laser as well as severely degrading the beam quality.

It is possible to reduce this problem by using two identical rods with a quartz rotator placed between them.[6] However, slight differences between the two rods will not be corrected and will still degrade beam quality. It is also possible to use birefringent laser crystals such as YLF or $YAlO_3$.[7] With these laser crystals the non-uniform thermally induced stress birefringence is a small fraction of the natural birefringence. However, these materials have other drawbacks. One significant problem in high power applications is that they are subject to fracture at significantly lower stress levels compared to YAG.

Stress depolarization can be avoided if the principal axes of the induced birefringence are confined to Cartesian rather than polar coordinates. This is exactly what is done in a slab geometry with one dimensional heat flow. In addition, for aspect ratios (slab width to thickness) greater than 2, the slab geometry has better thermal handling capabilities; the stress fracture limit is higher.[5]

A slab geometry laser has inherent advantages over the rod design. Previous analysis has assumed an ideal slab, where the slab is uniformly pumped over the large faces and only these two large faces of the slab are cooled.[5,8] In this case, it is possible to make a "plane-strain approximation" which reduces the problem to a simpler two-dimensional problem. All end effects are ignored in this analysis. By cooling only these two surfaces, heat flow is confined to one direction. The isotherms are then parallel to the y-z plane of the slab. Since the incident beam is usually polarized along the y-axis of the slab due to Brewster angle incidence, it does not suffer from stress depolarization. Stress birefringence is avoided by using a rectangular slab geometry with one dimensional heat flow.

There is still a temperature gradient in the slab due to the thermal loading. This again leads to a quadratic temperature profile and would lead to thermal lensing for a beam propagating straight through the gain medium. In fact, the thermal lens in a straight-through slab is twice that in a rod for an equivalent thermal load.[4] However, this thermal lens can be corrected by using a zig-zag optical path. In a zig-zag slab laser, the beam traverses the slab by bouncing between the two pumped faces. The thermal profile is symmetric about the center of the slab, so both the thermal lensing and thermal stresses are averaged to zero by the zig-zag path. In an ideal zig-zag slab laser, there is no thermal lensing or stress induced birefringence to first order. It is for these reasons that we have chosen to use a zig-zag slab design in our laser.

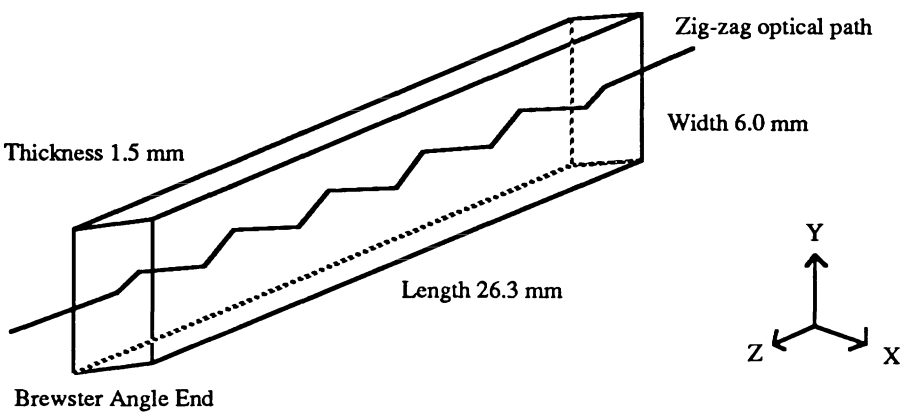

Figure 1: Diagram showing a typical slab geometry medium with a zig-zag optical path. The axes are indicated on the diagram for reference. Dimensions shown are for the Stanford Nd:YAG slab laser.

Of course, the ideal slab does not exist. When building a slab laser, end and edge effects act to degrade the beam quality. The performance of previous slab lasers has suffered from the inability to uniformly pump the slab, which resulted in beam distortions. In actual use, edge effects prevent the full aperture of the slab medium from being used, which limits the efficiency of slab lasers. However, by using optical fibers to pump the slab, our design has the flexibility to adjust the pump density and thermal loading in order to minimize these distortions. By adjusting the fiber distribution appropriately, it is possible to reduce problems due to end and edge effects. We have developed a series of computer programs which model the full three-dimensional behavior of the slab medium allowing us to examine the distortions in the slab due to the thermal loading. The aim of the computer analysis is to optimize the fiber distribution and thus to obtain the minimum wavefront distortion.

The computer modeling consists of three programs. The first program computes the heat loading in the slab for a given fiber position distribution. The second program uses finite element analysis to compute the temperature distribution and stresses in the slab. The third program propagates a wavefront through the slab to calculate the wavefront distortions caused by the original thermal load. Fiber positions were adjusted to minimize the uncorrectable single pass wavefront distortion.

As expected, the computer modeling shows that the zig-zag path averages the distortion in the x-direction. However, there is a slight cylindrical lens in the y-direction of the slab due to temperature differences across the width of the slab. In the computer model, the sides of the slab were insulated, creating this temperature distribution. It is possible to add temperature controllers on the sides of the slab, which should correct this lensing. The best single-pass wavefront to date was obtained by using an "orange grove" configuration of fibers. The fibers act as local hot spots on the slab due to the high intensity levels at the fiber output. To obtain a uniform wavefront, the local distortion seen by different portions of the beam must be equal after traversing the full slab length. Both edge-to-edge and top-to-bottom differences must be minimized by the fiber placement. Although the fibers are regularly spaced when viewed off axis, like the trees in an orange grove, the beam sees a uniform density of fibers as it travels the length of the slab. This arrangement closely simulates a uniformly pumped slab, even though a very localized pump source was used.

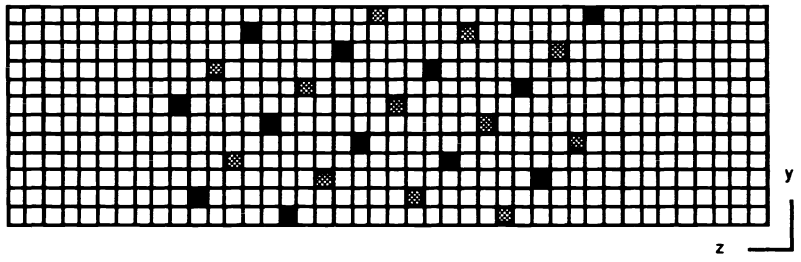

Figure 2: Diagram showing the "orange grove" configuration of fibers. Shaded boxes represent fiber positions with the different shading used to indicate fibers located on opposite sides of the slab. Grid shown is that used for finite element analysis.

Before closing this section, it is worthwhile to comment on the choice of slab dimensions. When choosing the size of the slab, there is a trade off between thermal considerations and gain. In a pulsed system it is possible to use a large slab volume since the high peak pump powers lead to large gains. This simplifies design since the thermal loads for a given power are much less in a large slab volume. For our cw laser, gain is critical and we must maximize the pump density. Ideally we would want the pumped slab volume to be as small as possible, but this is subject to thermal stress limits. If the slab thickness is too small, very little pump power will be absorbed in the active medium. We have chosen a slab with a thickness of 1.5 mm such that a double pass represents roughly one absorption length.

It is possible to reduce the thermal load by increasing the width or length of the slab. The thermal fracture limit of a slab depends on the aspect ratio of the slab and so a wider slab would seem better. However, the gain decreases as the slab width is increased, since the pump power is spread over a larger area. We have chosen a slab with an aspect ratio of 4, giving a width of 6 mm. The length we have chosen is 26.3 mm, end to end. It is possible to increase the length while still retaining the same gain-length product. However, tolerances on the slab surface are very critical due to the zig-zag optical path and so we have chosen dimensions which can be fabricated within the necessary tolerances.

As mentioned previously, the Stanford laser will have a total pump power of 250 watts. Due to the quantum defect of Nd:YAG, at least one quarter of this pump power will be dissipated as heat in the crystal. However, a more conservative rule of thumb when designing the laser is to assume that any pump power not removed as output power heats the crystal. The thermal loading in the crystal may be as high as 200 watts. This is a severe thermal load due to the small size of the Nd:YAG slab and we know we are near the stress fracture limit of YAG. At these thermal loads, the full three dimensional analysis that we have done is necessary. Our results show that even at these high thermal loads, the slab laser will outperform rod designs for efficient fundamental mode

operation. The slab geometry design will allow scaling to even higher average power levels since the power scales as the area of the slab.

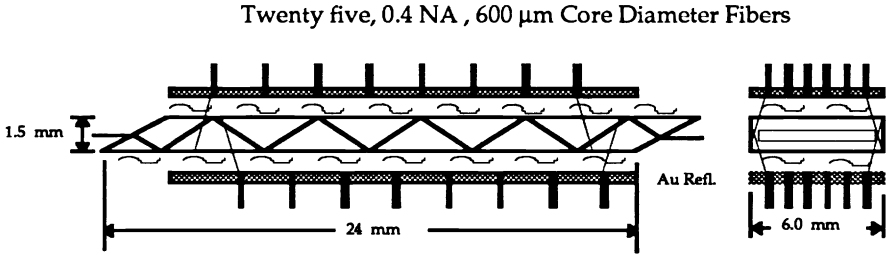

Figure 3: Diagram showing the pump and cooling configuration of the Stanford slab laser. The laser will be pumped from both sides. The large surfaces will be water cooled.

To summarize, slab geometry lasers have much better thermal handling characteristics than rod lasers. Not only is their thermal fracture limit higher, but stress birefringence problems are eliminated by using a rectilinear geometry with one dimensional heat flow. By using a zig-zag optical path, thermal lensing can be corrected in a uniformly-pumped ideal slab. The high thermal load in our slab leads to higher order effects in the slab, which have been modeled using a three dimensional finite element analysis computer program. This computer modeling indicates that the slab design will work well even at these power levels. We must now consider how to efficiently extract this pump energy from the slab laser medium.

3. RESONATOR DESIGN

For efficient near TEM_{00} mode operation, careful consideration must be given to the resonator design. To achieve single-frequency operation and avoid spatial hole burning, the resonator used will be a bow-tie ring cavity. Unidirectional operation is forced through injection locking rather than by using an intracavity optical diode. Injection locking avoids adding intracavity elements which increase cavity losses. In addition, injection locking allows us to actively stabilize the laser frequency. A 300 milliwatt laser will be used as the injection source. Locking of high power lasers has been demonstrated with slave to master oscillator power ratios as high as 200:1.[9] The high power slave laser should have a linewidth of 10 kHz, equal to that of the master oscillator.

For efficient energy extraction, a cavity mode with similar dimensions to the pumped area is required. The largest mode size easily obtained with a standard stable cavity has a waist in the range of 300 to 400 μm. This size provides sufficient overlap for the thin 1.5 mm x-direction, but is much too small for efficient energy extraction in the wide 6 mm y-direction. Because of the size and aspect ratio of the gain medium, we have chosen to use a stable-unstable resonator design. The cavity will be stable in the 1.5 mm x-direction and unstable in the 6 mm y-direction. When designing the laser cavity, we can design the stable and unstable directions of the cavity independently. By using cylindrical optics as mirrors in the ring cavity, we are able to shape the beam to obtain the desired spot size and aspect ratio in the Nd:YAG slab.

The resonator design is shown in figure 4. In the stable direction, we have a gain medium that is 1.5 mm thick with an 85% clear aperture. In standard rod designs, the cavity mode is chosen by rule of thumb to be roughly one-third to one-quarter of the rod diameter.[10] A large mode is desired to obtain a better overlap with the active gain region, but if the mode becomes too large, clipping at the edges decreases the laser performance. An intensity clipping level of 0.1% to 1% is usually chosen as a trade off between these competing criteria. This provides some mode selectivity due to intensity clipping at the gain medium edges but keeps the clipping losses for the fundamental TEM_{00} mode small. We can apply the same design consideration to the slab laser cavity. For our slab laser, the thin slab dimension is roughly the correct size to act as an aperture for the standard 300 to 400 μm spot size. We have designed the laser cavity to have a stable cavity mode in the x-direction of the slab with a waist of 340 μm. To avoid operating near the edge of stability, as is usually the case for large mode sizes, our ring laser cavity was designed with a focus in the arm opposite the gain medium. This design gives us a stable cavity away from the stability edge and a large mode in the gain region. These effects should give reliable operation in a TEM_0 gaussian mode for the stable resonator direction.

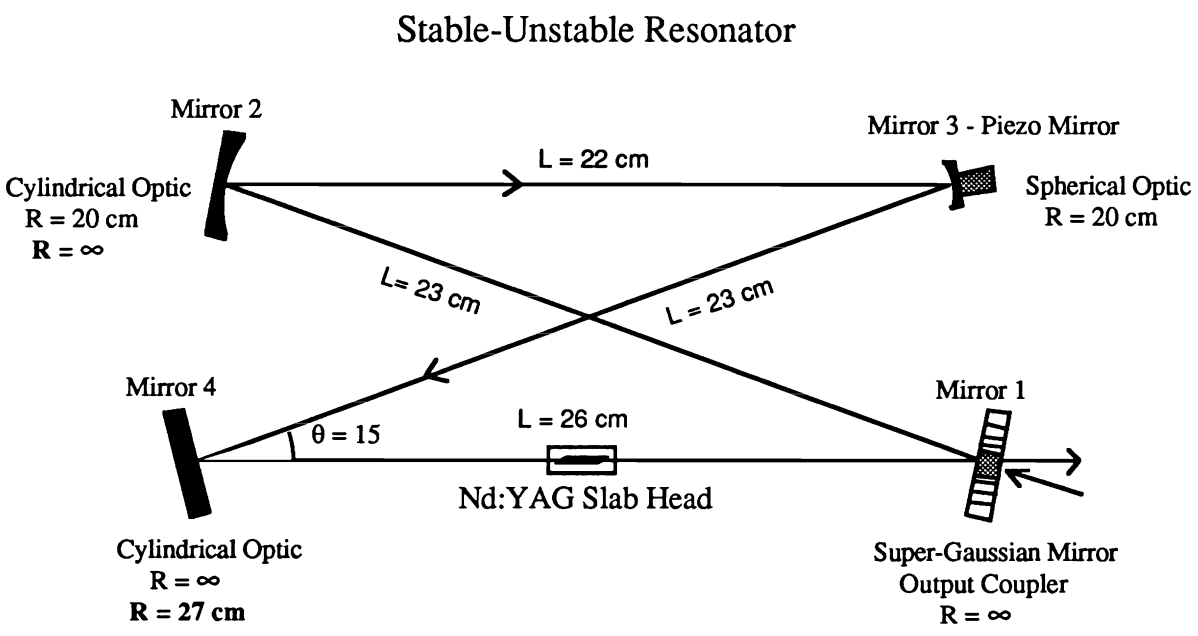

Figure 4: Diagram showing mirror curvatures and dimensions for the stable-unstable resonator. The tangential direction is stable, sagittal direction is unstable. Boldface curvatures refer to sagittal direction of cavity.

To obtain a large mode size in the y-direction of the slab an unstable resonator (UR) will be used. An unstable resonator allows for a large cavity mode with good selectivity against higher order transverse modes.[11] The earliest unstable resonators used for solid-state lasers were hard-edged UR.[12] These cavities had "polka-dot mirrors" that were highly reflective and used diffractive output coupling around the edges of these mirrors. The cavity mode size was adjusted by changing the diameter of these cavity mirrors. Large mode sizes could be obtained by suitable choices of the mirror diameters. The performance of these resonators depended on the magnification of the cavity resonators, with the best performance obtained in high gain, high magnification systems. One deleterious effect of this output coupling scheme was that diffractive coupling led to poor beam quality, with a spot of Arago in the near field and diffraction rings in the far field. A high magnification system contained more energy in the central lobe which led to better beam quality. However, large gain systems were necessary for the large magnification resonators since the output coupling was very high.

Variable reflectivity mirrors (VRM) have been developed to improve the beam quality of the output in unstable resonators. By tapering the reflectivity over a few Fresnel zones, diffraction effects are reduced. The first solid-state laser with a variable reflectivity mirror had a Gaussian reflectivity profile.[13,14] However, Gaussian VRMs cannot support a large mode without suffering from diffraction effects at the edges of the gain medium. The cavity mode for a Gaussian variable reflectivity mirror is also a Gaussian. As in the stable cavity, this mode cannot be chosen to be much greater than one-third the gain size without suffering from diffractive effects due to the gain edges. It is possible to overcome these limitations by using Super-Gaussian reflectivity mirrors (SGM).[15,16] A super-Gaussian profile has the form

$$R(r) = R_0 \exp\left[-2\left|\frac{r}{\omega_m}\right|^n\right],$$

where R_0 is the peak central reflectivity, ω_m is the mirror spot size and n is the order of the super-Gaussian profile. For n=2 we have a standard Gaussian profile and for $n=\infty$ we obtain a hard-edged profilem, i.e. a top-hat. By choosing values for n between these two extremes, super-Gaussian VRMs combine the advantages of both the hard-edged UR and the variable reflectivity profile. A large mode filling almost the entire gain region can be obtained without suffering from significant diffraction effects.

There are a number parameters which must be selected when designing a stable-unstable VRM resonator. These include the resonator magnification M, the central reflectivity R_0 of the SGM as well as the order of the super-Gaussian profile n. The SGM spot size ω_m must also be chosen, which determines the cavity spot size ω_i. In the next few paragraphs we will motivate our design choices for these parameters. Beam quality is the major design goal motivating our choices for these design parameters.

In a general unstable resonator, a large magnification is desired. The value of the magnification factor M determines both the mode discrimination ratio and the angular misalignment sensitivity. Better performance is obtained for both as M is increased. Typical choices for M in high gain lasers are between 1.5 and 3. The first hard-edged unstable resonators were designed with values of M at the higher end of this range since this increased the energy in the central lobe and decreased the energy in the diffraction rings. However, the output coupling of an unstable resonator depends on the magnification. For large magnification, a high gain system is needed, otherwise the laser will be overcoupled. For the one dimensional unstable resonator in our design, the geometric output coupling T is

$$T = 1 - \frac{R_0}{M}.$$

For a super-Gaussian mirror, the output beam quality also depends on the magnification. Both beam quality and the limited gain of our system favor low magnification in our laser design. However, the laser does run the risk of running in a stable mode due to residual focusing errors if the magnification is made too small.

Since the super-Gaussian mirror acts as the output coupler, the output beam will not have the same profile as the cavity mode. The cavity mode for a resonator using a super-Gaussian mirror can be solved analytically.[15] The cavity mode is super-Gaussian with the same order as the super-Gaussian mirror. However, the output of the cavity is this super-Gaussian mode multiplied by the transmission profile of the mirror. The output beam profile depends on the choice of R_0 and M. If the central reflectivity is too large or the magnification is large, the output beam profile will have a dip in the central region. Specifically, a dip in the output beam is obtained when $R_0M^n>1$. A maximally flat beam is obtained when

$$R_0M^n = 1.$$

In figure 5, we show the output beam profile for the conditions when $R_0M^n>1$, $R_0M^n=1$, and $R_0M^n<1$. The magnification was the only parameter changed to obtain these plots.

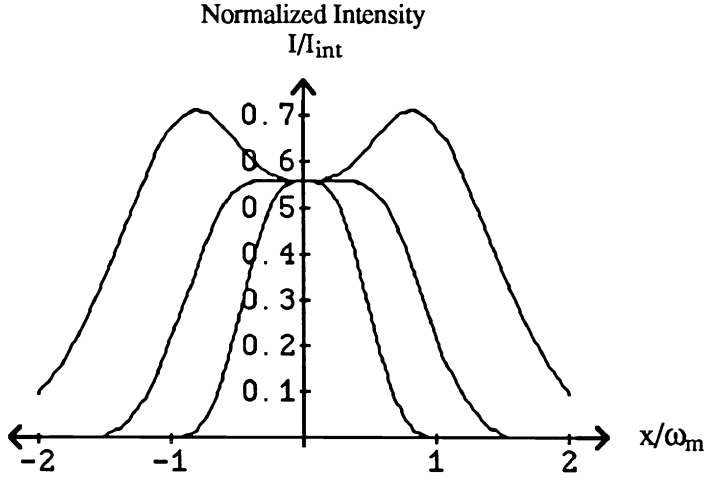

Figure 5: Diagram showing the output beam profile for transimission of the cavity mode through the super-Gaussian mirror. The profiles shown, from the outside in, are for the conditions $R_0M^n>1$, $R_0M^n=1$, and $R_0M^n<1$.

A reasonable magnification of M=1.5 and a low order super-Gaussian profile with n=3 results in a maximally flat condition for R_0=0.3. This gives an output coupling fraction T=77%. The system would need a

large gain to be able to operate with this much output coupling. In order to avoid overcoupling the laser with such a high output coupling fraction, one can accept a dip in the output beam profile by increasing R_0, or decrease the value of M. We have chosen slab dimension which maximize the gain but have a thermal load under the stress fracture limit. This gain allows a large output coupling fraction. We have also chosen to work at low magnification to minimize the dip in the output beam profile.

Before choosing values of R_0, M and n, it is important to look at the output power as a function of output coupling fraction. We have estimated the small signal gain in our laser to be just under 2. If we apply the Rigrod analysis, we find that the output power is insensitive to the value of T, assuming a fixed cavity loss.[17] In our design, we can choose values for T between T=0.2 and T=0.7 without a significant change in output power. For reasonable cavity loss values, the output power changes by only 5 to 15% over this range. This allows us to design a resonator which is overcoupled without suffering a significant loss in output power. Combining this fact with the maximally flat beam condition, we obtain limits on the choice of the magnification,

$$1.25 < M^{n+1} < 4.$$

This confines our choice of both n and M if we wish to obtain a good quality beam. A larger n will favor output power and efficiency over beam quality. A larger M will increase the cavity misalignment tolerance but will again decrease beam quality. We have chosen to use relatively small values for n and M, while reducing cavity losses as much as possible to increase output power and efficiency. Of course, maximum efficiency is obtained by minimizing the cavity losses.

Using the above condition, it is possible to plot values of R_0 versus M for different values of n. The same can be done for the output coupling T. We have chosen to slightly overcouple the laser in order to improve the overall performance. Beam quality is improved since we can lower R_0 for a given combination of n and M. Again, this should not decrease output power significantly according to the Rigrod analysis. The results of this analysis led us to choose a super-Gaussian profile with n=4 and R_0=0.46 with a cavity magnification of M=1.35.

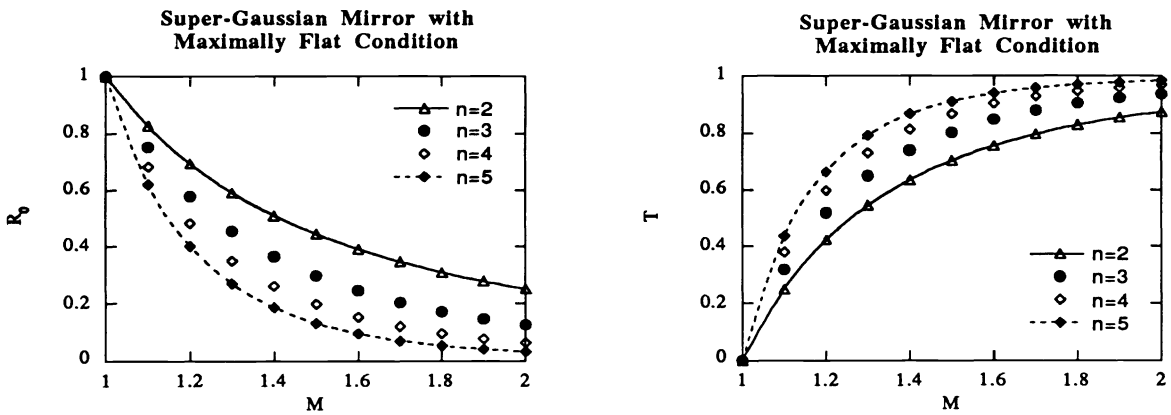

Figure 6: Plots showing the possible values of peak reflectivity R_0 (left) and mirror transmission T (right) for a given magnification M and super-Gaussian order n.

The last parameters to be chosen for the super-Gaussian mirror and the unstable resonator are the mirror spot size and cavity spot size. These two parameters are related by the equation[16]

$$\omega_i = \omega_m (M^n - 1)^{1/n}.$$

To obtain a good overlap with the gain, the cavity spot size, ω_i, should be chosen to match the gain size while still avoiding diffraction at the edges. We have chosen a cavity spot size ω_i=2.2 mm and a mirror spot size ω_m=2.0 mm. Mirrors 3 and 4 in the cavity determine the magnification in the unstable direction.

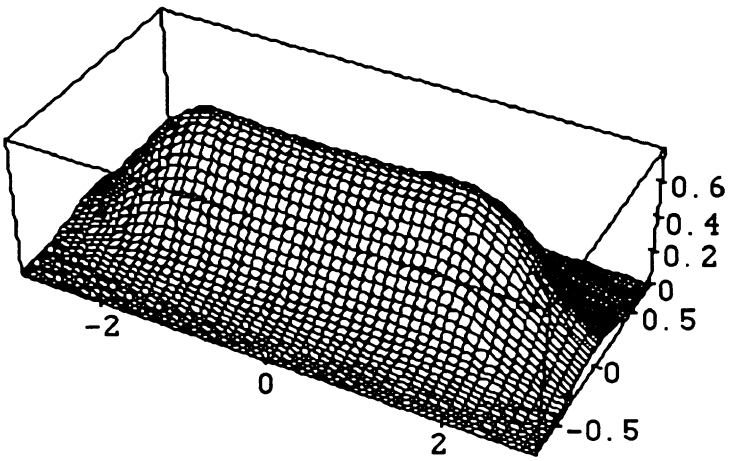

Figure 7: Diagram showing the predicted output beam for the design parameters chosen for the Stanford Nd:YAG slab laser. Units for x and y directions are mm with the boxed area equal to the slab diemensions. The z dimension is plotted as normalized intensity, I/I_{int}.

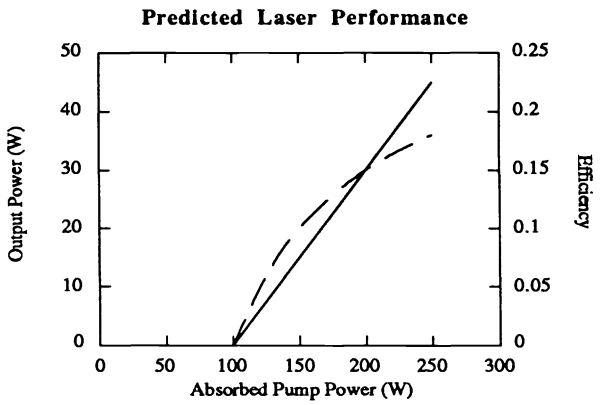

Figure 8: Predicted laser performance of Stanford Nd:YAG slab laser. Both ouput power (solid line) and efficiency (dashed line) are shown. Graph was obtained by assuming 5% roundtrip cavity loss.

Using the calculated stable-unstable cavity mode, we have calculated an overlap integral to obtain an estimated slope efficiency for the laser.[18] These results indicate that the slope efficiency should be near 30% in the fundamental mode. This calculated efficiency is comparable to slope efficiencies obtained with previous slab lasers in multimode operation. A graph showing the predicted laser performance is shown in figure 8.

4. Conclusion

The design goal of our project is to design and build a 50 watt cw, single-frequency, fundamental mode solid-state laser. We chose to use a slab laser design for its improved thermal loading characteristics relative to a rod. We have developed a series of computer programs to model the three-dimensional effects in the slab caused by the

extreme thermal loading. The pump distribution was selected to minimize the wavefront distortion of a beam passing through the slab. We have also designed a stable-unstable resonator to efficiently extract the pump power in a single-frequency fundamental mode. By using a super-Gaussian mirror unstable resonator we can obtain a large mode size in a high quality beam. We have chosen the following parameters for the mirror:

R_0 (central reflectivity) = 0.46
n (super-Gaussian order) = 4
ω_m (mirror spot size) = 2.0 mm
M (cavity magnification) = 1.35

The calculated slope efficiency is 30%. With the 250 watts of diode pump power, we expect to obtain 50 watts cw in a single-frequency, diffraction-limited, fundamental mode.

5. ACKNOWLEDGMENTS

This work is supported by the Defense Advanced Research Projects Agency (DARPA), contract number DAAL03-90-C-2026. The authors would like to thank Alex Farinas and Yushi Kaneda for interesting and useful discussions.

6. REFERENCES

1. A. Abramovici, W.E. Althouse, R.W.P. Drever, Y. Gursel, S. Kawamura, F.J. Raab, D. Shoemaker, L. Sievers, R.E. Spero, K.P. Thorne, R.E. Vogt, R. Weiss, S.E. Whitcomb and M.E. Zucker, "LIGO: The Laser Interferometer Gravitational-Wave Observatory," Science, 256, pp. 325-333, 1992.

2. Spectra Diode Laboratory product literature, part number SDL-3450-P5

3. W.F. Krupke, M.D. Shinn, J.E. Marion, J.A. Caird, and S.E. Stokowski, "Spectroscopic, optical, and thermomechanical properties of neodymium- and chromium-doped gadolinium scandium gallium garnet," J.O.S.A. B, 3, pp. 102-113, 1986.

4. W. Koechner, Solid-State Laser Engineering, 3rd ed., Ch. 7, Springer-Verlag, New York, 1992.

5. J.M. Eggleston, T.M. Kane, K. Kuhn, J. Unternahrer and R.L. Byer, "The Slab Geometry Laser--Part 1: Theory," IEEE J.Q.E, Q.E.-20, pp. 289-301, 1984.

6. S.C. Tidwell, J.F. Seamans, M.S. Bowers, and A.K. Cousins, "Scaling CW Diode-End-Pumped Nd:YAG Lasers to High Average Power," IEEE J.Q.E, 28, pp. 997-1009, 1992.

7. W. Koechner, p.399.

8. T.J. Kane, J.M. Eggleston and R.L. Byer, "The Slab Geometry Laser--Part II: Thermal Effects in a Finite Slab," IEEE J.Q.E., Q.E.-21, pp. 1195-1210, 1985.

9. C.D. Nabors, A.D. Farinas, T. Day, S.T. Yang, E.K. Gustafson and R.L. Byer, "Injection locking of a 13 W cw Nd:YAG ring laser," Opt. Lett., 14, pp. 1189-1191, 1989.

10. V. Magni, "Resonators for solid-state lasers with large-volume fundamental mode and high alignment stability," Appl. Opt., 25, pp. 107-117, 1986.

11. A.E. Siegman, Lasers, Ch. 22-23, University Science Books, Mill Valley (CA), 1986.

12. R.L. Herbst, H. Komine, and R.L. Byer, "A 200 mJ unstable resonator Nd:YAG oscillator," Opt. Commun., 21, pp. 5-7, 1977.

13. G. Giuliani, Y.K. Park, and R.L. Byer, "Radial Birefringent Element and its Application to Laser Resonator Design," Opt. Lett., 5, pp. 491-493, 1980.

14. J. Eggleston, G. Guiliani, and R.L. Byer, "Radial Intensity Filters using Radial Birefringent Elements," JOSA, 71, pp. 1264-1271, 1981.

15. S. DeSilvestri, P. Laporta, V. Magni, and O. Svelto, "Solid-State Laser Unstable Resonators with Tapered Reflectivity Mirrors: The Super-Gaussian Approach," IEEE J.Q.E., Q.E.-24, pp. 1172-1177, 1988.

16. S. DeSilvestri, V. Magni, O. Svelto, and G. Valentini, "Lasers with Super-Gaussian Mirrors," IEEE J.Q.E., Q.E.-26, pp. 1500-1509, 1990.

17. W.W. Rigrod, "Saturation effects in high-gain lasers," J. Appl. Phys., 36, pp. 2487-2490, 1965.

18. K. Kubodera and K. Otsuka, "Single-transverse-mode $LiNdPO_4$ slab waveguide laser," J. Appl. Phys., 50, pp. 653-659, 1979.